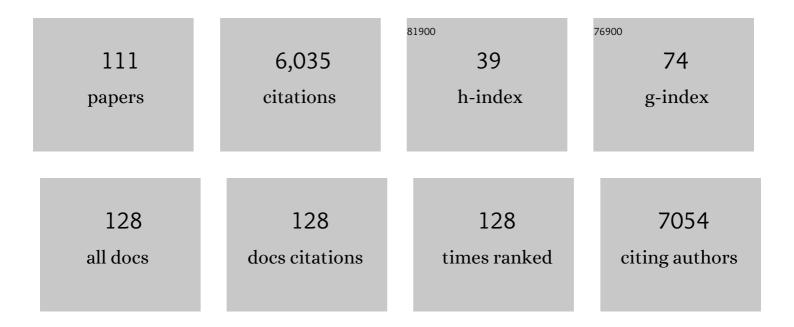
Catherine Ottlé

List of Publications by Year in descending order

Source: https://exaly.com/author-pdf/7805471/publications.pdf Version: 2024-02-01



#	Article	IF	CITATIONS
1	Quantifying and Reducing Uncertainty in Global Carbon Cycle Predictions: Lessons and Perspectives From 15ÂYears of Data Assimilation Studies With the ORCHIDEE Terrestrial Biosphere Model. Global Biogeochemical Cycles, 2022, 36, .	4.9	8
2	Modeling subgrid lake energy balance in ORCHIDEE terrestrial scheme using the FLake lake model. Geoscientific Model Development, 2022, 15, 4275-4295.	3.6	2
3	Irrigation, damming, and streamflow fluctuations of the Yellow River. Hydrology and Earth System Sciences, 2021, 25, 1133-1150.	4.9	19
4	Evaluating and Optimizing Surface Soil Moisture Drydowns in the ORCHIDEE Land Surface Model at In Situ Locations. Journal of Hydrometeorology, 2021, 22, 1025-1043.	1.9	10
5	Variance Based Sensitivity Analysis of FLake Lake Model for Global Land Surface Modeling. Journal of Geophysical Research D: Atmospheres, 2021, 126, e2019JD031928.	3.3	3
6	Optimizing Lake Surface Water Temperature Simulations Over Large Lakes in China With FLake Model. Earth and Space Science, 2021, 8, e2021EA001737.	2.6	12
7	Characterization of SWOT Water Level Errors on Seine Reservoirs and La Bassée Gravel Pits: Impacts on Water Surface Energy Budget Modeling. Remote Sensing, 2020, 12, 2911.	4.0	4
8	Improved Nearâ€Surface Continental Climate in IPSLâ€CM6Aâ€LR by Combined Evolutions of Atmospheric and Land Surface Physics. Journal of Advances in Modeling Earth Systems, 2020, 12, e2019MS002005.	3.8	36
9	Presentation and Evaluation of the IPSLâ€CM6A‣R Climate Model. Journal of Advances in Modeling Earth Systems, 2020, 12, e2019MS002010.	3.8	541
10	Modeling Land Surface Fluxes from Uncertain Rainfall: A Case Study in the Sahel with Field-Driven Stochastic Rainfields. Atmosphere, 2020, 11, 465.	2.3	1
11	Deceleration of China's human water use and its key drivers. Proceedings of the National Academy of Sciences of the United States of America, 2020, 117, 7702-7711.	7.1	155
12	Improvement of the Irrigation Scheme in the ORCHIDEE Land Surface Model and Impacts of Irrigation on Regional Water Budgets Over China. Journal of Advances in Modeling Earth Systems, 2020, 12, e2019MS001770.	3.8	15
13	Implementation of the CMIP6 Forcing Data in the IPSL M6A‣R Model. Journal of Advances in Modeling Earth Systems, 2020, 12, e2019MS001940.	3.8	95
14	Evaluation of global terrestrial evapotranspiration using state-of-the-art approaches in remote sensing, machine learning and land surface modeling. Hydrology and Earth System Sciences, 2020, 24, 1485-1509.	4.9	130
15	Testing water fluxes and storage from two hydrology configurations within the ORCHIDEE land surface model across US semi-arid sites. Hydrology and Earth System Sciences, 2020, 24, 5203-5230.	4.9	16
16	Confronting Soil Moisture Dynamics from the ORCHIDEE Land Surface Model With the ESA-CCI Product: Perspectives for Data Assimilation. Remote Sensing, 2018, 10, 1786.	4.0	18
17	Evaluation of ORCHIDEE-MICT-simulated soil moisture over China and impacts of different atmospheric forcing data. Hydrology and Earth System Sciences, 2018, 22, 5463-5484.	4.9	13
18	Contributions of Climate Change, CO2, Land-Use Change, and Human Activities to Changes in River Flow across 10 Chinese Basins. Journal of Hydrometeorology, 2018, 19, 1899-1914.	1.9	24

#	Article	IF	CITATIONS
19	The Indian-French Trishna Mission: Earth Observation in the Thermal Infrared with High Spatio-Temporal Resolution. , 2018, , .		27
20	Inversion of Surface Soil Moisture from Radar Altimetry Backscattering in Semi-Arid Environments. , 2018, , .		0
21	Partitioning global land evapotranspiration using CMIP5 models constrained by observations. Nature Climate Change, 2018, 8, 640-646.	18.8	219
22	ORCHIDEE-MICT (v8.4.1), aÂland surface model for the high latitudes: model description and validation. Geoscientific Model Development, 2018, 11, 121-163.	3.6	135
23	The impact of typhoons on sediment connectivity: lessons learnt from contaminated coastal catchments of the Fukushima Prefecture (Japan). Earth Surface Processes and Landforms, 2017, 42, 306-317.	2.5	65
24	Testing the capability of <scp>ORCHIDEE</scp> land surface model to simulate <scp>A</scp> rctic ecosystems: Sensitivity analysis and siteâ€level model calibration. Journal of Advances in Modeling Earth Systems, 2017, 9, 1212-1230.	3.8	9
25	Variational assimilation of land surface temperature within the ORCHIDEE Land Surface Model Version 1.2.6. Geoscientific Model Development, 2017, 10, 85-104.	3.6	3
26	Evaluating the performance of land surface model ORCHIDEE-CANÂv1.0 on water and energy flux estimation with a single- and multi-layer energy budget scheme. Geoscientific Model Development, 2016, 9, 2951-2972.	3.6	43
27	A multi-layer land surface energy budget model for implicit coupling with global atmospheric simulations. Geoscientific Model Development, 2016, 9, 223-245.	3.6	51
28	Rainfall Intra-Seasonal Variability and Vegetation Growth in the Ferlo Basin (Senegal). Remote Sensing, 2016, 8, 66.	4.0	14
29	Downscaling Meteosat Land Surface Temperature over a Heterogeneous Landscape Using a Data Assimilation Approach. Remote Sensing, 2016, 8, 586.	4.0	7
30	Data Assimilation of Satellite Observations. , 2016, , 357-382.		1
31	Causes of uncertainty in China's net primary production over the 21st century projected by the <scp>CMIP5</scp> Earth system models. International Journal of Climatology, 2016, 36, 2323-2334.	3.5	14
32	Plant functional type classification for earth system models: results from the European Space Agency's Land Cover Climate Change Initiative. Geoscientific Model Development, 2015, 8, 2315-2328.	3.6	197
33	Land surface temperature retrieval over circumpolar Arctic using SSM/l–SSMIS and MODIS data. Remote Sensing of Environment, 2015, 162, 1-10.	11.0	51
34	Spring snow cover deficit controlled by intraseasonal variability of the surface energy fluxes. Environmental Research Letters, 2015, 10, 024018.	5.2	26
35	Impacts of Satellite-Based Snow Albedo Assimilation on Offline and Coupled Land Surface Model Simulations. PLoS ONE, 2015, 10, e0137275.	2.5	16
36	Improving the dynamics of Northern Hemisphere high-latitude vegetation in the ORCHIDEE ecosystem model. Geoscientific Model Development, 2015, 8, 2263-2283.	3.6	36

#	Article	IF	CITATIONS
37	Genetic particle filter application to land surface temperature downscaling. Journal of Geophysical Research D: Atmospheres, 2014, 119, 2131-2146.	3.3	19
38	The influence of local spring temperature variance on temperature sensitivity of spring phenology. Global Change Biology, 2014, 20, 1473-1480.	9.5	90
39	Genetic Particle Smoother thermal sharpener: Methodology and application to pseudo-observations. , 2014, , .		0
40	Surface Temperature Downscaling From Multiresolution Instruments Based on Markov Models. IEEE Transactions on Geoscience and Remote Sensing, 2013, 51, 1588-1612.	6.3	14
41	The MISTIGRI thermal infrared project: scientific objectives and mission specifications. International Journal of Remote Sensing, 2013, 34, 3437-3466.	2.9	52
42	Tracking the early dispersion of contaminated sediment along rivers draining the Fukushima radioactive pollution plume. Anthropocene, 2013, 1, 23-34.	3.3	90
43	Automatic detection of field furrows from very high resolution optical imagery. International Journal of Remote Sensing, 2013, 34, 3467-3484.	2.9	4
44	Use of various remote sensing land cover products for plant functional type mapping over Siberia. Earth System Science Data, 2013, 5, 331-348.	9.9	24
45	Evolution of radioactive dose rates in fresh sediment deposits along coastal rivers draining Fukushima contamination plume. Scientific Reports, 2013, 3, 3079.	3.3	51
46	Evaluation of an improved intermediate complexity snow scheme in the ORCHIDEE land surface model. Journal of Geophysical Research D: Atmospheres, 2013, 118, 6064-6079.	3.3	63
47	Response to Comment on "Surface Urban Heat Island Across 419 Global Big Cities― Environmental Science & Technology, 2012, 46, 6889-6890.	10.0	15
48	Surface Urban Heat Island Across 419 Global Big Cities. Environmental Science & Technology, 2012, 46, 696-703.	10.0	864
49	Land Surface Temperature product validation using NOAA's surface climate observation networks—Scaling methodology for the Visible Infrared Imager Radiometer Suite (VIIRS). Remote Sensing of Environment, 2012, 124, 282-298.	11.0	101
50	Spatio-temporal surface soil heat flux estimates from satellite data; results for the AMMA experiment at the Fakara (Niger) supersite. Agricultural and Forest Meteorology, 2012, 154-155, 55-66.	4.8	26
51	Analysis of vegetation seasonality in Sahelian environments using MODIS LAI, in association with land cover and rainfall. Journal of Arid Environments, 2012, 84, 38-50.	2.4	34
52	State-dependent errors in a land surface model across biomes inferred from eddy covariance observations on multiple timescales. Ecological Modelling, 2012, 246, 11-25.	2.5	18
53	Land water storage variability over West Africa estimated by Gravity Recovery and Climate Experiment (GRACE) and land surface models. Water Resources Research, 2011, 47, .	4.2	76
54	Controls on winter ecosystem respiration in temperate and boreal ecosystems. Biogeosciences, 2011, 8, 2009-2025.	3.3	42

#	Article	IF	CITATIONS
55	Remote sensing of the land surface during the African Monsoon Multidisciplinary Analysis (AMMA). Atmospheric Science Letters, 2011, 12, 129-134.	1.9	12
56	Multi-model comparison of a major flood in the groundwater-fed basin of the Somme River (France). Hydrology and Earth System Sciences, 2010, 14, 99-117.	4.9	40
57	A New Land Surface Hydrology within the Noah-WRF Land-Atmosphere Mesoscale Model Applied to Semiarid Environment: Evaluation over the Dantiandou Kori (Niger). Advances in Meteorology, 2009, 2009, 1-13.	1.6	9
58	The AMMA Land Surface Model Intercomparison Project (ALMIP). Bulletin of the American Meteorological Society, 2009, 90, 1865-1880.	3.3	165
59	ERS scatterometer surface soil moisture analysis of two sites in the south and north of the Sahel region of West Africa. Journal of Hydrology, 2009, 375, 253-261.	5.4	20
60	Water and energy budgets simulation over the AMMA-Niger super-site spatially constrained with remote sensing data. Journal of Hydrology, 2009, 375, 287-295.	5.4	56
61	The AMMA-CATCH experiment in the cultivated Sahelian area of south-west Niger – Investigating water cycle response to a fluctuating climate and changing environment. Journal of Hydrology, 2009, 375, 34-51.	5.4	114
62	SEtHyS_Savannah: A multiple source land surface model applied to Sahelian landscapes. Agricultural and Forest Meteorology, 2009, 149, 1421-1432.	4.8	23
63	Monitoring land surface processes with thermal infrared data: Calibration of SVAT parameters based on the optimisation of diurnal surface temperature cycling features. Remote Sensing of Environment, 2008, 112, 872-887.	11.0	29
64	Canopy bidirectional reflectance calculation based on Adding method and SAIL formalism: AddingS/AddingSD. Remote Sensing of Environment, 2008, 112, 3639-3655.	11.0	17
65	Fusion of Vegetation Indices Using Continuous Belief Functions and Cautious-Adaptive Combination Rule. IEEE Transactions on Geoscience and Remote Sensing, 2008, 46, 1499-1513.	6.3	9
66	Subpixel Temperature Estimation from Low Resolution Thermal Infrared Remote Sensing. , 2008, , .		2
67	Canopy Bidirectional Reflectance Calculation based on adding method and SAIL formalism. , 2007, , .		2
68	Soil moisture mapping based on ASAR/ENVISAT radar data over a Sahelian region. International Journal of Remote Sensing, 2007, 28, 3547-3565.	2.9	62
69	An improved SVAT model calibration strategy based on the optimisation of surface temperature temporal dynamics. Geophysical Research Letters, 2007, 34, .	4.0	17
70	Determination of vegetation cover fraction by inversion of a four-parameter model based on isoline parametrization. Remote Sensing of Environment, 2007, 111, 553-566.	11.0	47
71	FLuorescence EXplorer (FLEX): an optimised payload to map vegetation photosynthesis from space. , 2006, , .		9
72	Contribution of Thermal Infrared Remote Sensing Data in Multiobjective Calibration of a Dual-Source SVAT Model. Journal of Hydrometeorology, 2006, 7, 404-420.	1.9	41

#	Article	IF	CITATIONS
73	Land cover change detection at coarse spatial scales based on iterative estimation and previous state information. Remote Sensing of Environment, 2005, 95, 464-479.	11.0	35
74	Future directions for advanced evapotranspiration modeling: Assimilation of remote sensing data into crop simulation models and SVAT models. Irrigation and Drainage Systems, 2005, 19, 377-412.	0.5	98
75	Constraining a physically based Soil-Vegetation-Atmosphere Transfer model with surface water content and thermal infrared brightness temperature measurements using a multiobjective approach. Water Resources Research, 2005, 41, .	4.2	43
76	Using a multiobjective approach to retrieve information on surface properties used in a SVAT model. Journal of Hydrology, 2004, 287, 214-236.	5.4	61
77	Land surface temperature retrieval techniques and applications. , 2004, , .		22
78	Surface soil moisture estimation from the synergistic use of the (multi-incidence and) Tj ETQq0 0 0 rgBT /Overlock Environment, 2003, 86, 30-41.	10 Tf 50 5 11.0	547 Td (mul 73
79	Sequential Assimilation ofERS-1SAR Data into a Coupled Land Surface–Hydrological Model Using an Extended Kalman Filter. Journal of Hydrometeorology, 2003, 4, 473-487.	1.9	81
80	Mesh size selection in a soil-biosphere-atmosphere transfer model. Journal of Environmental Engineering and Science, 2003, 2, 77-81.	0.8	1
81	Multi-scale data fusion using Dempster-Shafer evidence theory. Integrated Computer-Aided Engineering, 2003, 10, 9-22.	4.6	37
82	Comparison of measured and SISPAT-RS simulated brightness temperatures and reflectances at field scale during ReSeDA experiment. , 2002, 4542, 130.		0
83	Integration of remote sensing data into hydrological models for reservoir management. Hydrological Sciences Journal, 2002, 47, 159-161.	2.6	1
84	Modélisation hydro-météorologique du bassin du Rhône : apport de la télédétection spatiale. Houill Blanche, 2002, 88, 57-61.	e 0.3	1
85	Conversion of 400-1100 nm vegetation albedo measurements into total shortwave broadband albedo using a canopy radiative transfer model. Agronomy for Sustainable Development, 2002, 22, 611-618.	0.8	18
86	Monitoring energy and mass transfers during the Alpilles-ReSeDA experiment. Agronomy for Sustainable Development, 2002, 22, 597-610.	0.8	21
87	Effect of aerodynamic resistance modelling on SiSPAT-RS simulated surface fluxes. Agronomy for Sustainable Development, 2002, 22, 641-650.	0.8	7
88	SVAT modeling over the Alpilles-ReSeDA experiment: comparing SVAT models over wheat fields. Agronomy for Sustainable Development, 2002, 22, 651-668.	0.8	32
89	Quelques applications de la télédétection à la physique des surfaces continentales. Annales Des Telecommunications/Annals of Telecommunications, 2001, 56, 617-631.	2.5	0
90	Hydro-meteorological modelling of the Rhone basin: general presentation and objectives. Physics and Chemistry of the Earth, 2001, 26, 443-453.	0.3	8

#	Article	IF	CITATIONS
91	IRSUTE. Remote Sensing of Environment, 1999, 68, 357-369.	11.0	62
92	Further Insights into the Use of the Split-Window Covariance Technique for Precipitable Water Retrieval. Remote Sensing of Environment, 1999, 69, 84-86.	11.0	4
93	The ISBA surface scheme in a macroscale hydrological model applied to the Hapex-Mobilhy area. Journal of Hydrology, 1999, 217, 75-96.	5.4	103
94	The ISBA surface scheme in a macroscale hydrological model applied to the Hapex-Mobilhy area. Journal of Hydrology, 1999, 217, 97-118.	5.4	43
95	Simulation of the water budget and the river flows of the Rhone basin. Journal of Geophysical Research, 1999, 104, 31145-31172.	3.3	76
96	Analytical parameterization of canopy directional emissivity and directional radiance in the thermal infrared. Application on the retrieval of soil and foliage temperatures using two directional measurements. International Journal of Remote Sensing, 1997, 18, 2587-2621.	2.9	123
97	Estimation of total atmospheric water vapor content from split-window radiance measurements. Remote Sensing of Environment, 1997, 61, 410-418.	11.0	24
98	Atmospheric corrections in the thermal infrared: global and water vapor dependent split-window algorithms-applications to ATSR and AVHRR data. IEEE Transactions on Geoscience and Remote Sensing, 1996, 34, 457-470.	6.3	72
99	Introduction of the soil/vegetation/atmosphere continuum in a conceptual rainfall/runoff model. Hydrological Sciences Journal, 1996, 41, 889-902.	2.6	34
100	Thermal remote sensing of land surface temperature from satellites: Current status and future prospects. International Journal of Remote Sensing, 1995, 12, 175-224.	1.0	208
101	Evaluation of the ERS 1/Synthetic Aperture Radar Capacity to Estimate Surface Soil Moisture: Two-Year Results Over the Naizin Watershed. Water Resources Research, 1995, 31, 975-982.	4.2	53
102	Estimation of the angular variation of the sea surface emissivity with the ATSR/ERS-1 data. Remote Sensing of Environment, 1994, 48, 302-308.	11.0	16
103	Assimilation of soil moisture inferred from infrared remote sensing in a hydrological model over the HAPEX-MOBILHY region. Journal of Hydrology, 1994, 158, 241-264.	5.4	121
104	Effect of atmospheric absorption and surface emissivity on the determination of land surface temperature from infrared satellite data. International Journal of Remote Sensing, 1993, 14, 2025-2037.	2.9	82
105	Estimation of land surface temperature with NOAA9 data. Remote Sensing of Environment, 1992, 40, 27-41.	11.0	113
106	Use of thermal infrared remote sensing for water budget studies. Advances in Space Research, 1991, 11, 163-167.	2.6	4
107	Introduction of a Realistic Soil-Vegetation Component in a Hydrological Model: Application to HAPEX-MOBILHY Experiment. , 1991, , 137-144.		2
108	Application of satellite remote sensing to estimate areal evapotranspiration over a watershed. Journal of Hydrology, 1990, 121, 321-333.	5.4	17

#	Article	IF	CITATIONS
109	Remote sensing applications to hydrological modeling. Journal of Hydrology, 1989, 105, 369-384.	5.4	32
110	Multi-scale data fusion using Dempster-Shafer evidence theory. , 0, , .		11
111	Surface soil moisture estimation using active microwave ERS wind scatterometer and SAR data. , 0, , .		0